ALEPH 92-106
PHYSIC 92-95
G. Cowan
8.7.1992

Update on Sub-jet Multiplicities in Hadronic Z Decays

Glen D. Cowan
MPI Munich
July 8, 1992

Abstract

This note describes an analysis of sub-jet multiplicities in hadronic Z decays. The measurements are based on charged particles from approximately 300000 hadronic events at a center-of-mass energy of $E_{cm} = 91.2$ GeV. First, two-jet and three-jet event samples are selected using the Durham clustering algorithm with a value of the jet-resolution cut-off, y_1. These event samples are then analyzed separately with the same jet algorithm using a smaller cut-off, y_0. The mean number of clusters (sub-jet multiplicity) as a function of y_0 is compared to recently available perturbative QCD calculations [1]. The measurements are also compared to the predictions of Monte Carlo hadron production models. Significant differences between models are seen in the perturbative region, indicating sensitivity to higher order effects in the parton shower.

This note is an update of ALEPH 92-85 and is to be made available for conference speakers. It is intended as the basis for a publication. Please send comments to vxcrna::cowan.

1. Introduction

The large number of events of the type $e^+e^- \rightarrow hadrons$ available from the ALEPH experiment at LEP provides an opportunity to investigate the detailed structure of hadronic final states. Of foremost importance are measurements which allow a direct comparison with the predictions of QCD. In this note, measurements are made of sub-jet multiplicities in two-jet and three-jet samples. The results are compared with recently available perturbative QCD calculations [1], which are sensitive to the gluon self-coupling and to soft gluon interference effects. In addition, the measurements are compared to the hadron level predictions of Monte Carlo models, where a significant discrimination between competing models is found.

The number of jets in an event is defined with a "JADE type" clustering algorithm [2]. For each pair of particles in the event, one defines the quantity y_{ij} (the Durham metric [3])

$$y_{ij} = \frac{2min(E_i^2, E_j^2)(1 - cos\theta_{ij})}{E_{vis}^2} , \tag{1}$$

where E_i is the energy of particle i, θ_{ij} is the angle between the pair, and E_{vis} is the visible energy in the event. The pair with the smallest value of y_{ij} is replaced by a pseudoparticle (cluster). The four-momentum of the cluster is taken to be the sum of the four momenta of particles i and j (the "E" recombination scheme). The procedure is repeated until all of the y_{ij} are greater than a given threshold, y_{cut} (the jet resolution parameter). The number of jets is defined to be the number of remaining clusters.

First, two and three jet events are selected using an initial value of the resolution parameter, y_1. The mean sub-jet multiplicity, $M_{2(3)}$, for the two (three) jet sample is then determined as a function of a smaller value of the resolution parameter, y_0. Since the jet multiplicities depend logarithmically on the resolution parameter, it is also convenient to introduce the variables

$$L_{0(1)} = -\ln y_{0(1)} \tag{2}$$

which are used in the following in addition to y_0 and y_1.

The two-jet sample consists predominantly of an initial $q\bar{q}$ system followed by soft gluon radiation, whereas the three-jet sample is enriched by events with a single hard (high $k_\perp$) gluon. The initial $q\bar{q}$ or $q\bar{q}g$ system continues to radiate gluons as shown in figure 1. The quark-gluon coupling is proportional to the QCD color factor $C_F = 4/3$, whereas the gluon-gluon coupling is proportional to $C_A = 3$. Thus one expects the three jet sample to have a higher rate of increase in sub-jet multiplicity as a function of y_0 than the two-jet sample. For asymptotically high energies (and correspondingly small y_0) one expects

$$R = \frac{M_3 - 3}{M_2 - 2} \rightarrow \frac{2C_F + C_A}{2C_F} = \frac{17}{8} . \tag{3}$$

Note that the ratio as defined here is equivalent to M_3/M_2, examined in reference [1], in the limit that the multiplicities are large. The advantage of subtracting the initial number of jets is in the increased sensitivity in the region where y_0 is close to y_1 (i.e. M_2 only slightly larger than two, M_3 only slightly larger than three).

In fact, the sub-jet enhancement in the three-jet sample is measured to be much smaller than expected from color-charge counting arguments. Discrepancies between the observed properties of gluon jets and the naive expectations have been observed in the reaction $e^+e^- \rightarrow hadrons$ at LEP [4] and also at lower energies [5]. In reference [1] it is shown that soft gluon interference effects play an important role at presently accessible energies. When these are taken into account, QCD in fact predicts a much smaller enhancement in the sub-jet multiplicity for three-jet events.

2. Experimental method

The measurements presented here are based on the charged particles measured by the Time Projection Chamber (TPC) and the Inner Tracking Chamber (ITC) of the ALEPH detector [6]. Charged tracks were required to have at least four three-dimensional coordinates from the TPC, to extrapolate to within 2 cm of the beam line and to within 5 cm of the origin in the direction along the beam. In addition, the angle with respect to the beam was required to be at least 20 degrees, and the transverse momentum component relative to the beam had to be at least 200 MeV/c. Using tracks which met these criteria, the sphericity axis and the total charged energy were computed. Events were required to have at least five accepted charged tracks, the polar angle of the sphericity axis, θ_{sph}, in the range $35° \leq \theta_{sph} \leq 145°$, and a total charged energy of at least 15 GeV. This event selection yielded a sample of approximately 300000 hadronic events with center-of-mass energies in the range 91.0 GeV $\leq E_{cm} \leq$ 91.5 GeV.

The measurments have been corrected for effects of geometrical acceptance, detector efficiency and resolution, decays, secondary interactions and initial state photon radiation by the following procedure. A first set of hadronic events with flavor composition as predicted by the Standard Model was generated using the Lund Parton-Shower model (PS) [11] including initial state photon radiation. The events were passed through the detector simulation program to produce simulated raw data, which were then processed through the same reconstruction and analysis chain as the real data. A second set of Monte Carlo data without detector simulation was generated, in which all particles with mean lifetimes less than 1 ns were required to decay, the others were treated as stable, and initial state radiation was turned off. These two data sets were used to derive multiplicative correction factors for the *additional* number of jets resolved when going to a jet resolution parameter y_0 smaller than the initial value y_1. The corrected sub-jet multiplicity in the n-jet sample, $n = 2, 3$, is given by

$$(M_n(y_0) - n)_{corrected} = (M_n(y_0) - n)_{measured} \cdot C(y_0) \tag{4}$$

where

$$C(y_0) = \frac{(M_n - n)_{MC\ generator\ only}}{(M_n - n)_{MC\ gen.+detector\ sim.}} \tag{5}$$

This procedure corrects the measurements back to a fixed center-of-mass energy (free of initial state radiation) and a well defined final state particle composition that can be compared directly to model calculations. The correction factors are typically in the range $1.00 \leq C \leq 1.12$. Correction factors for $M_2 - 2$ and $M_3 - 3$ for $L_1 = 3$ are shown in figure 2.

The correction factors have been computed so as to take into account charged particles only. This is to minimize systematic errors when comparing with the charged particle predictions of Monte Carlo models. One can also construct the corrections so as to measure what the jet multiplicity would be if both charged and neutral particles are measured. Monte Carlo studies indicate that this quantity would not differ much from the charged only case for sufficiently large y_0, since the jet resolution parameter is normalized to the visible energy in the event. This can be seen in figure 3, where the measured charged particle jet multiplicities are shown with the predictions of the Lund PS model (JETSET) for charged particles only, charged and neutral particles, and partons. The charged and neutral hadron jet multiplicities agree with those from charged only to within 10% for $y_0 \geq 10^{-4}$. For smaller y_0, individual particles (eventually even those from decays) are resolved, and the jet multiplicity tends toward the mean number of particles in the event sample. For the charged particles the asymptotic value is around 20, whereas for charged and neutral, it is about twice as much.

In order to estimate the systematic uncertainty from the generator dependence of the correction factors, approximate factors were derived from several Monte Carlo models, discussed below. For these, only the previously described cuts were applied to the generated events, which can be accomplished much more quickly than processing the events through the full detector simulation. As can be seen from figure 2, the approximate correction factors reproduce the overall form of the factors using the full simulation, and they differ among each other by typically less than 1% to 2%.

It was checked that the corrected jet multiplicities are not sensitive to the event and track selection criteria by varying all of the cuts. No evidence for a systematic dependence was found beyond the one percent level.

Based on the studies of the generator dependence of the correction factors and variation of the cuts, an overall systematic error of 2% is assigned to the sub-jet multiplicities. This is conservative for small y_0, where the sub-jet multiplicity tends toward the charged particle multiplicity for the event sample in question. (In reference [7] it has been shown that the mean charged multiplicity is measured in ALEPH with a systematic error of about 1.2%.) For the ratio $R = (M_3 - 3)/(M_2 - 2)$, the systematic errors largely cancel. The remaining systematic error is conservatively estimated to be around 1%. On all plots the quadratic sum of statistical and systematic uncertainties is shown.

3. Comparison with perturbative QCD

In comparing the hadron level measurements directly with parton level QCD predictions, one checks the combined assumption of QCD and Local Parton Hadron Duality (LPHD), i.e. the assumption that hadronic jets follow their partonic ancestors. The QCD predictions from reference [1] are only expected to be valid for sufficiently large L_1 (small y_1). Figure 4 shows the measured sub-jet multiplicities for $L_1 = 5$ ($y_1 = 0.00674$) compared to the QCD predictions. Both $M_2 - 2$ and $M_3 - 3$ are in good qualitative agreement with the QCD prediction in the perturbative region ($y_0 \geq 10^{-4}$). For smaller y_0, the QCD prediction eventually diverges, whereas the measured multiplicity tends toward the charged particle multiplicity of the event sample.

One may also examine the ratio $R = (M_3 - 3)/(M_2 - 2)$ which is expected to be less sensitive to non-perturbative effects than the absolute multiplicities. The ratio is shown in figure 5 along with the QCD prediction. For purposes of comparison one may evaluate the QCD prediction from reference [1] with $C_A = C_F = 4/3$, i.e. with the quark and gluon color charges set equal. As can be seen from figure 5, this "toy" theory shows a less rapid rise in R as y_0 is decreased. The fact that the ratio is substantially smaller than the asymptotic value of equation (3) is attributed to gluon interference effects (angular ordering), which decrease the width of the rapidity plateau of sub-jets in a gluon jet [1].

To further investigate the role of coherence in $(M_3 - 3)/(M_2 - 2)$, the following incoherent model has been proposed [8]. For M_3, a three parton system is generated according to the first order matrix element, giving values of $x_q, x_{\bar{q}}$ and x_g, where $x_i = 2E_i/E_{cm}$. Each parton is assumed to radiate according to its energy, without interference:

$$\begin{aligned} M_2 &= 2N_q(E_{cm}) \,, \\ M_3 &= N_q(x_q E_{cm}) + N_q(x_{\bar{q}} E_{cm}) + N_g(x_g E_{cm}) \,, \end{aligned} \tag{6}$$

where the parton multiplicities from quark and gluon jets, N_q and N_g, are computed in reference [9]. As can be seen from figure 5, the incoherent model gives a significantly higher value of $(M_3 - 3)/(M_2 - 2)$.

4. Comparison with Monte Carlo Models

As can be seen from figure 3, non-perturbative effects become important for values of y_0 less than 10^{-3} to 10^{-4}. Monte Carlo hadron production models which include a perturbative part to generate a system of partons followed by a non-perturbative mechanism to convert the partons into hadrons should, in principle, describe the data over the entire range of y_0. Here, five such models are considered: the Lund Parton Shower model (JETSET) version 7.2 [10], [11], HERWIG version 5.4 [13], ARIADNE version 4.02 [14], COJETS version 6.23 [15], and NLLjet version 2.0 [16]. (For a review of event generators see, for example, reference [17].) The important parameters of the models have been tuned using ALEPH data on charged particle inclusive and event shape distributions [12]. (For COJETS, the parameters were left at their default values, derived by the model's authors from comparison to a variety of LEP and lower energy data.)

Although the perturbative levels of all the models are equivalent to leading order, there are many differences in the treatment of sub-leading effects. For example, the choice of evolution parameter for the Altarelli-Parisi equation, the argument of the splitting kernels, the argument of $\alpha_s(Q^2)$ and the implementation of soft gluon interference effects differ from model to model. Three of the models, JETSET, ARIADNE and NLLjet, use the Lund string mechanism for the hadronization. Therefore any difference in the predictions of these models is related to the perturbative level. HERWIG uses cluster fragmentation and COJETS uses independent fragmentation. The basic features of the models are described in appendix A.

Figures 6 and 7 show the mean number of additional sub-jets for the two and three jet samples, $M_2 - 2$ and $M_3 - 3$, for $L_1 = 3$ ($y_1 = 0.0498$) and $L_1 = 5$ ($y_1 = 0.00674$) with the predictions of the Monte Carlo models. Shown in figures 8 and 9 are the ratios of model predictions to measured values. Although all of the models qualitatively reproduce the measured values, the ratios of model to data clearly indicate differing levels of agreement.

Consider, for example, the two-jet sample selected with $L_1 = 3$ (figures 6*a* and 8*a*). The main contribution to M_2 comes from soft gluon radiation from the initial quark-antiquark pair; i.e. no gluon was emitted that was hard enough to be resolved at the scale y_1. As can be seen in figure 8*a*, all of the models (except COJETS) are in agreement with the data to within 5% over the entire range of y_0.

For the three-jet sample, however, the level of agreement with models is quite different, as can be seen in figures 6*b* and 8*b*. Recall that M_3 is sensitive to soft gluon radiation from the hard gluon as well as that from the quark and antiquark. For small y_0, all of the models agree with the data to within a few percent. This is not surprising, since the parameters of the models have been tuned to reproduce the mean charged multiplicity, i.e. the sub-jet multiplicity in the limit of vanishing y_0.

In the perturbative region ($y_1 \geq 10^{-3}$), however, discrepancies between models and data are as large as 30%. HERWIG is in the best agreement with the data until the region of y_0 very close to y_1, where the prediction is too high. The statistical errors are very large in this region, however, and the the discrepancy is only about two standard deviations. ARIADNE is also in very good agreement with the data.

The discrepancies in M_3 between models and data become smaller when L_1 is increased, as shown in figure 9*b*. This is not surprising, since the three-jet sample then becomes more two-jet like. It appears that that all models can adequately describe soft gluon radiation from the quark and antiquark, but differ in their description of soft gluon radiation from a hard gluon.

Figures 10 and 11 show the ratio of additional sub-jets in the three-jet sample to that for the two-jet sample, $R = (M_3 - 3)/(M_2 - 2)$, for $L_1 = 3, 5$. Here again one sees a certain disagreement amoung the models in the perturbative region. ARIADNE gives the best description of the data. In the non-perturbative region, the data and the

model predictions become flat. That is, the non-perturbative conversion of partons into hadrons appears to be similar for quarks and gluons.

5. Conclusions

The sub-jet multiplicities for two and three jet events have been measured and compared to theoretical predictions. A comparison with parton level QCD formula shows a clear indication for the higher color charge of the gluon. The sub-jet enhancement in the three-jet sample is substantially smaller than predicted by simple color-charge arguments, but is in qualitatively good agreement with a QCD calculation which takes into account interference effects.

A significant discrimination betwen competing Monte Carlo models is found, especially in the perturbative region. In particular, differing levels of agreement with the data were found for the three-jet sample, where a correct description of soft gluon radiation from a hard gluon is expected to be important. The models ARIADNE and HERWIG are found to provide the best description of the data.

Acknowledgements

Many thanks to B. R. Webber for numerous discussions as well as for computer code for the QCD predictions.

Appendix A: Description of Monte Carlo Models

Lund Parton Shower (JETSET version 7.2)

In the Lund Parton Shower (PS) model (program JETSET version 7.2, [11], [10]) the evolution of the parton system is treated as a probablistic branching process based on the leading logarithm approximation (LLA). In this picture partons undergo decays of the type $q \rightarrow qg$, $g \rightarrow gg$ and $g \rightarrow q\bar{q}$. The probability of a decay $a \rightarrow bc$ is given by the Altarelli-Parisi equation

$$\frac{d\mathcal{P}_{a \rightarrow bc}}{dt} = \int dz \frac{\alpha_s(Q^2)}{2\pi} P_{a \rightarrow bc}(z) \tag{7}$$

where the evolution parameter $t = \ln(Q^2_{evol}/\Lambda)$, $\alpha_s(Q^2)$ is the strong coupling constant evaluated at Q^2 equal to the transverse momentum squared of the branching. $P_{a \rightarrow bc}(z)$ are the Altarelli-Parisi splitting kernels, and the argument z is taken to be the first daughter's energy fraction in the center-of-mass frame, assuming massless daughters. The evolution parameter is computed from the virtual mass of the parent parton, $Q_{evol} = m_{parent}$, and the (effective) QCD scale parameter Λ.

For the first branchings of the initial quark and antiquark, a rejection technique is used so as to reproduce the $O(\alpha_s)$ three-jet cross section. Interference effects are included by requiring that the emission angles of successive branchings always decrease (angular ordering). Certain higher order effects are not included in the default version of the program (used here), such as the azimuthal distribution in gluon decays from spin and coherence effects. The parton shower is stopped when the parton virtualities drop below a pre-set cut-off, Q_0.

The conversion of the partons into hadrons is accomplished with the Lund String Model. Gluons are associated with momentum carrying kinks in the string. Hadron production results from a breaking of the string which can be interpreted as virtual quark-antiquark pair production in a flux-tube. The hadrons' transverse momenta are taken from a Gaussian distribution, and the longitudinal momenta are determined from a phenomenological fragmentation function.

The most important parameters were tuned using charged particle event-shape and inclusive distributions [12]. The values are:

Λ_{LLA}	PARJ(81)	0.318 GeV
M_{min}	PARJ(82)	1.43 GeV
σ	PARJ(21)	0.36 GeV
b	PARJ(42)	0.92 GeV^{-2}
a	PARJ(41)	0.50 (fixed at default)
ϵ_c	- PARJ(54)	0.020
ϵ_b	- PARJ(55)	0.015

HERWIG version 5.4

The HERWIG Monte Carlo (version 5.4) [13] is also based on a parton branching process as described above. Instead of the parton virtual mass for for the evolution paremeter, HERWIG uses $Q_{evol} = \zeta_a$ defined by

$$\begin{aligned} \zeta_a &= E_a\sqrt{\xi_{bc}}\ , \\ \xi_{bc} &= \tfrac{p_b \cdot p_c}{E_b E_c}\ , \end{aligned} \tag{8}$$

for the branching $a \rightarrow bc$ where p_b, p_c, E_b and E_c are the four-momenta and energies of partons b and c. Angular ordering of successive branchings is approximately equivalent to ordering of the ξ_{bc}. The argument z of the Altarelli-Parisi splitting kernels is taken to be the daughter's energy fraction, and the scale for the coupling α_s is the transverse momentum squared of the branching. Azimuthal asymmetries for gluon decays both from coherence and spin effects are included. Hard gluon emission is (approximately) taken into account in the most recent version (5.4) by partial inclusion of the first order matrix element.

The hadronization stage in HERWIG is accompished by a cluster mechanism. At the end of the parton shower, all gluons split into quark-antiquark pairs. Neighboring $q\bar{q}$ pairs form color neutral clusters which (usually) decay into two hadrons. The hadron type is determined by the available phase space. Special treatment is allowed for very light and very heavy clusters.

The model parameters were tuned using charged particle event-shape and inclusive distributions using the same technique as described in reference [12]. The values are:

Λ_{QCD}	QCDLAM	0.154 GeV
M_{gluon}	RMASS(13)	0.865 GeV
	VGCUT	0.0 (fixed)
$M_{max}^{cluster}$	CLMAX	3.65 GeV

COJETS version 6.23

The COJETS model [15] also uses the leading logarithm approximation to describe a cascade of successive parton branchings. The evolution variable for the Altarelli-Parisi equations as well as the argument of α_s are taken to be the parent parton's virtual mass. The argument of the Altarelli-Parisi splitting kernels is taken to be the fraction of $E + p_{||}$ of the daughter parton. Angular ordering is not included. The first parton branching is corrected so as to reproduce the $O(\alpha_s)$ approximation for single gluon emission. Since the model uses an independent fragmentation mechanism to convert the partons into hadrons, the parton shower must be cut-off at a comparatively high parton virtuality, 3 GeV. The parameters have been tuned by the model's author using data from LEP and from lower energies.

ARIADNE version 4.02

Instead of formulating the perturbative QCD cascade in terms of quark and gluon decays, the ARIADNE Monte Carlo [14] uses the complementary language of color dipoles. In this approach, the initially produced color dipole (the $q\bar{q}$ pair) radiates a gluon according to the first order QCD matrix element. The resulting $q\bar{q}g$ system is then treated as two independent dipoles, between the quark and gluon, and between the gluon and antiquark. Each successive gluon emission creates a new dipole, all of which are assumed to radiate independently. This approach naturally takes into account coherence effects, azimuthal dependence of gluon decays, and an exact $O(\alpha_s)$ description of hard gluon radiation which much be inserted by hand into the parton cascade approach used in Lund PS and HERWIG. Certain other ambiguities, however, are less straight forward to handle in the color dipole approach, such as how to absorb the recoils when a dipole emits a gluon, or how to include the creation of $q\bar{q}$ pairs in the cascade.

The non-perturbative hadron production in ARIADNE is accomplished with the Lund String model [10].

The model parameters were tuned using charged particle event-shape and inclusive distributions using the same technique as described in reference [12]. The values are:

Λ_{QCD}	PARA(1)	0.218 GeV
$p_\perp^{min}$	PARA(3)	0.69 GeV
σ	PARJ(21)	0.36 GeV
b	PARJ(42)	0.77 GeV^{-2}
a	PARJ(41)	0.50 (fixed at default)
ϵ_c	- PARJ(54)	0.050
ϵ_b	- PARJ(55)	0.006

NLLjet version 2.0

The NLLjet program [16] goes beyond the LLA to include next-to-leading logs. Here, parton branchings of the type $q\rightarrow qgg$, $q\rightarrow qq\bar{q}$, $g\rightarrow ggg$ and $g\rightarrow gq\bar{q}$ are included, as well as higher order corrections to the standard $1\rightarrow 2$ branchings. The evolution variable is based on the parent parton's virtuality, $Q_{evol} = m_{parent}$, and for a decay $a\rightarrow bc$ the argument of the splitting kernels is given by $z = (E_b + p_{||b})/(E_a + p_{||a})$. Angular ordering of succesive parton emissions is included.

The non-perturbative hadron production in NLLjet is accomplished with the Lund String model [10].

The model parameters were tuned using charged particle event-shape and inclusive distributions using the same technique as described in reference [12]. The values are:

Λ_{QCD}	LAMBDA	0.275 GeV
Q_0^2	Q02	0.807 GeV^2
σ	PARJ(21)	0.407 GeV
b	PARJ(42)	0.987 GeV^{-2}
a	PARJ(41)	0.50 (fixed at default)
ϵ_c	- PARJ(54)	0.050
ϵ_b	- PARJ(55)	0.006

References

[1] S. Catani, B.R. Webber, Yu.L. Dokshitzer, and F. Fiorani, CERN-TH.6419/92 (1992).

[2] W. Bartel et al., JADE Collaboration, Z. Phys. **C33** (1986) 23;
S. Bethke et al., JADE Collaboration, Phys.Lett. **B213** (1988) 235.

[3] Durham Workshop, W.J. Stirling, *J. Phys.* **G**: *Nucl. Part. Phys.* **17** (1991) 1567;
N. Brown and W.J. Stirling, *RAL preprint* **91-049** (1991);
S. Bethke, Z. Kunszt, D.E. Soper and W.J. Stirling, *CERN preprint* **TH.6221/91** (1991).

[4] G. Alexander et al., (OPAL) Phys. Lett. **B 265** (1991) 462.

[5] W. Bartel et al., (JADE) Phys. Lett. **123B** (1983) 460;
M. Derrick et al., (HRS) Phys. Lett. **165 B** (1985) 449;
A. Petersen et al., (Mark II) Phys. Rev. Lett. **55** (1985) 1954;
W. Braunschweig et al., (TASSO) Z. Phys. **C45** (1989) 1;
Y. K. Kim et al., (AMY) Phys Rev. Lett. **63** (1989) 1772.

[6] D. Decamp et al., Nucl. Instr. Meth. A **294** (1990) 121.

[7] D. Decamp et al., Phys. Lett. **B 273** (1991) 181.

[8] B. Webber, private communication.

[9] S. Catani, Yu. L. Dokshitzer, F. Fiorani and B.R. Webber, CERN-TH.6328/91 (1991).

[10] B. Andersson, G. Gustafson, G. Ingelman and T. Sjöstrand, Phys. Rep. **97** (1983) 31.

[11] M. Bengtsson and T. Sjöstrand, Phys. Lett. **185B** (1987) 435.

[12] D. Buskulic et al., (ALEPH) *Properties of Hadronic Z^0 Decays and Test of QCD Generators*, CERN-PPE/92-62.

[13] G. Marchesini and B.Webber, Cavendish-HEP-88/7 (1988);
G. Marchesini and B. Webber, Nucl. Phys. **B310** (1988) 461;
I. Knowles, Nucl. Phys. **B310** (1988) 571.

[14] L. Lönnblad, DESY 92-046 (1992).

[15] R. Odorico, DFUB 92-6 (1992).

[16] K. Kato and T. Munehisa, Computer Physics Communications **64** (1991) 67, Mod. Phys. Lett. **A 1** (1986) 345, Phys. Rev **D 36** (1987) 61, Phys. Rev. **D 39** (1989) 156.

[17] Z Physics at LEP I, Volume 3: Event Generators and Software, G. Altarelli, R. Kleiss and C. Verzegnassi, ed., CERN 89-08 (1989) 143.

Figure 1. (a) A two-jet event which emits soft gluon radiation with a coupling $C_F = 4/3$. (b) A three-jet event in which the hard gluon emits further gluons with a coupling $C_A = 3$.

Figure 2. Corrections factors for $L_1 = 3$ for $M_2 - 2$ (a) and $M_3 - 3$ (b). Also shown are approximate correction factors derived from several Monte Carlo models. The spread in the curves is an indication of the Monte Carlo generator dependence of the correction factors.

Figure 3. Corrected charged particle sub-jet multiplicities from ALEPH with the predictions of the Lund PS model. (a) M_2, $L_1 = 3$. (b) M_3, $L_1 = 3$. (c) M_2, $L_1 = 5$. (d) M_3, $L_1 = 5$. Also shown are the Lund PS predictions for all hadrons (charged and neutral) and for partons.

Figure 4. Charged particle sub-jet multiplicities for $L_1 = 5$ compared to parton level QCD predictions. (a) $M_2 - 2$. (b) $M_3 - 3$.

Figure 5. The ratio $(M_3 - 3)/(M_2 - 2)$ compared to the QCD prediction. Also shown are a "toy model" in which $C_A = C_F = 4/3$ and an incoherent model.

Figures 6. $M_2 - 2$ and $M_3 - 3$ for charged particles along with the predictions of Monte Carlo models for $L_1 = 3$.

Figures 7. $M_2 - 2$ and $M_3 - 3$ for charged particles along with the predictions of Monte Carlo models for $L_1 = 5$.

Figure 8. The ratios of model to data for $M_2 - 2$ and $M_3 - 3$ for $L_1 = 3$.

Figure 9. The ratios of model to data for $M_2 - 2$ and $M_3 - 3$ for $L_1 = 5$.

Figure 10. The ratio $(M_3 - 3)/(M_2 - 2)$ for $L_1 = 3$ compared to the predictions of Monte Carlo models.

Figure 11. The ratio $(M_3 - 3)/(M_2 - 2)$ for $L_1 = 5$ compared to the predictions of Monte Carlo models.

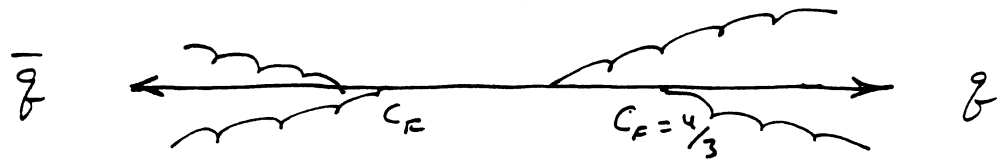

Figure 1a. Soft gluon radiation from a two-jet event.

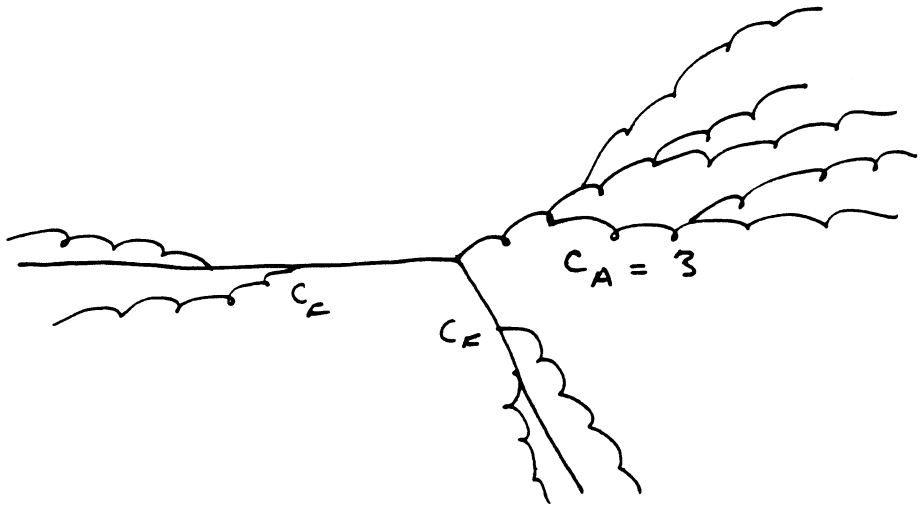

Figure 1b. Soft gluon radiation from a three-jet event

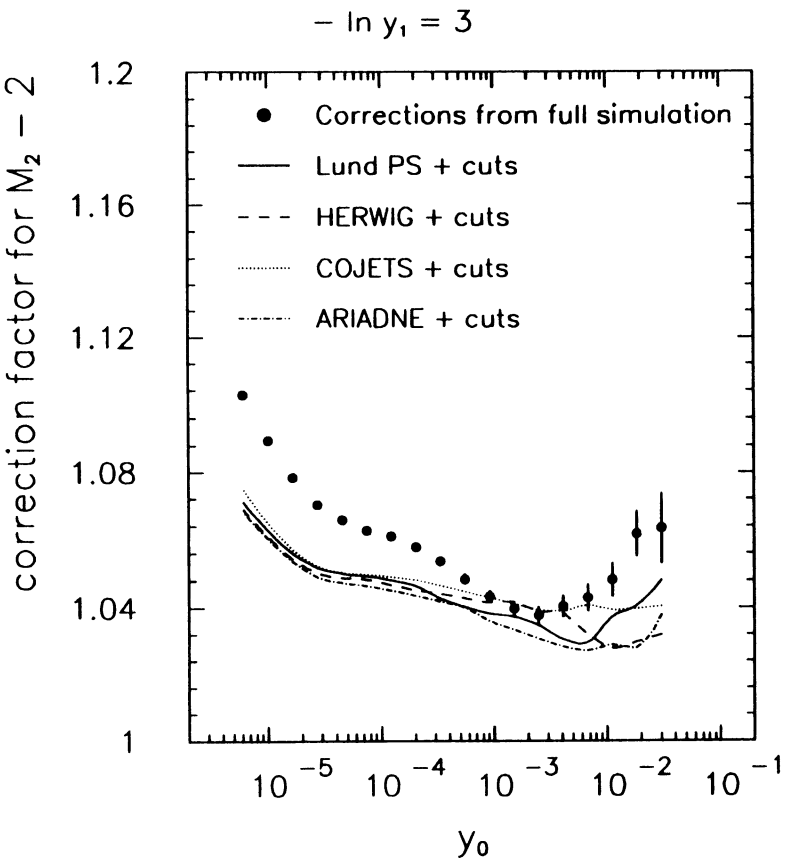
− ln y₁ = 3
correction factor for M₂ − 2
1.2
1.16
1.12
1.08
1.04
1
Corrections from full simulation
Lund PS + cuts
HERWIG + cuts
COJETS + cuts
ARIADNE + cuts
10 −5
10 −4
10 −3
10 −2
10 −1
y₀

Fig. 2a

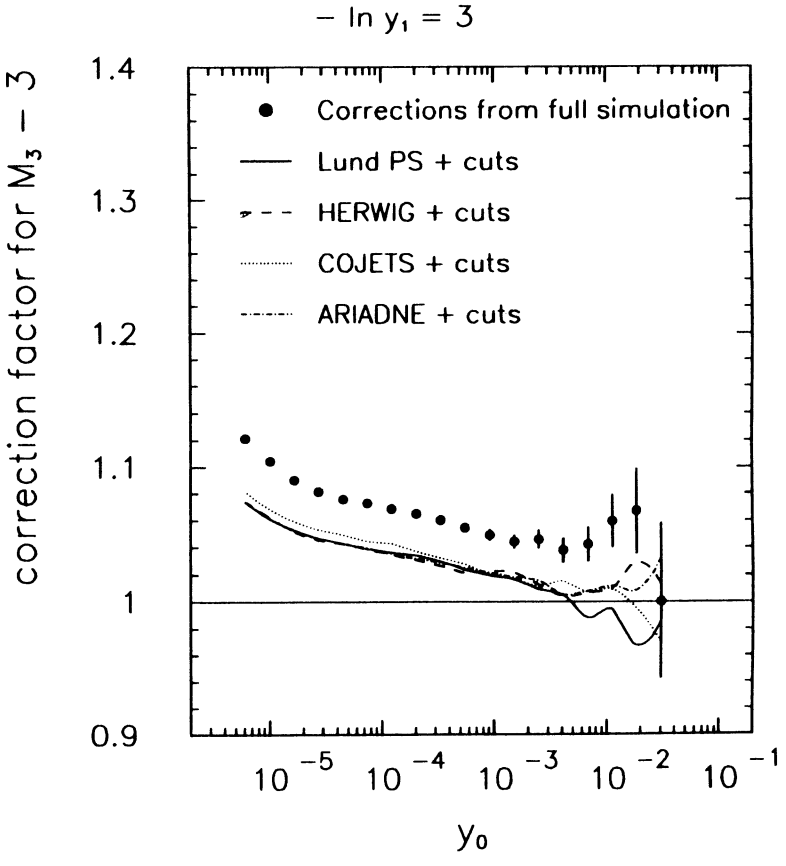
− ln y₁ = 3
correction factor for M₃ − 3
1.4
1.3
1.2
1.1
1
0.9
Corrections from full simulation
Lund PS + cuts
HERWIG + cuts
COJETS + cuts
ARIADNE + cuts
10 −5
10 −4
10 −3
10 −2
10 −1
y₀

Fig. 2b

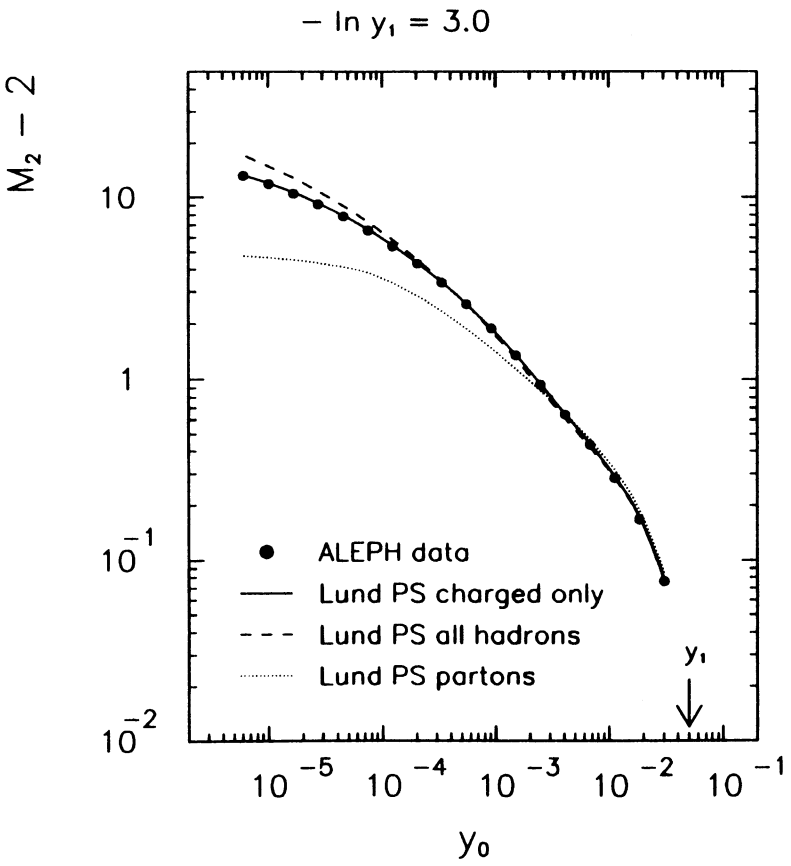
− ln y₁ = 3.0
M₂ − 2
10
1
10⁻¹
10⁻²
10⁻⁵ 10⁻⁴ 10⁻³ 10⁻² 10⁻¹
y₀
ALEPH data
Lund PS charged only
Lund PS all hadrons
Lund PS partons
y₁

Fig. 3a

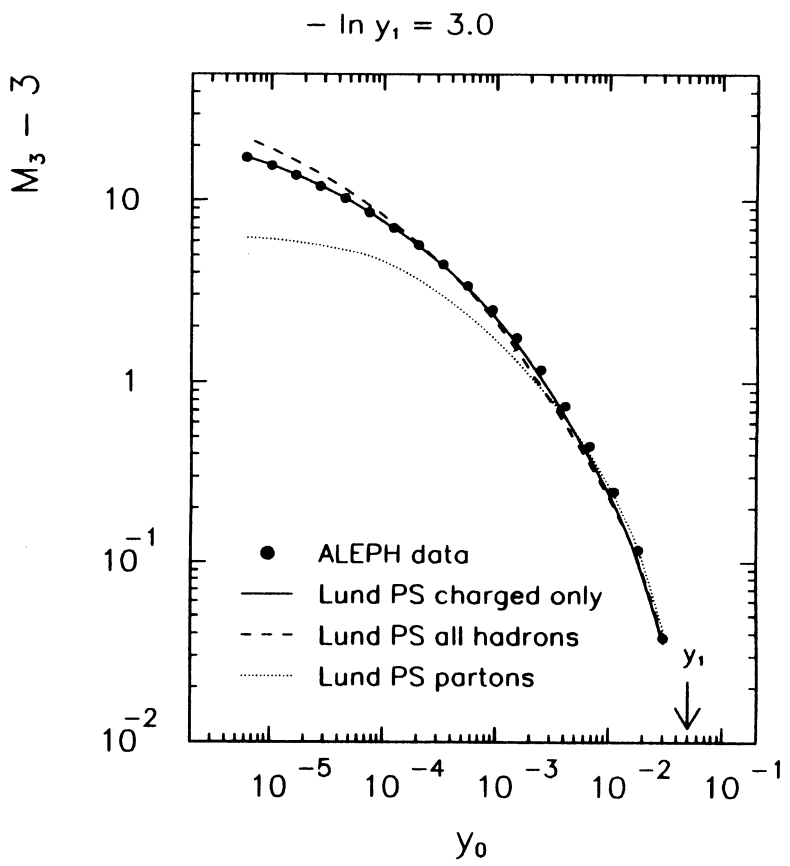
− ln y₁ = 3.0
M₃ − 3
10
1
10⁻¹
10⁻²
10⁻⁵ 10⁻⁴ 10⁻³ 10⁻² 10⁻¹
y₀
ALEPH data
Lund PS charged only
Lund PS all hadrons
Lund PS partons
y₁

Fig. 3b

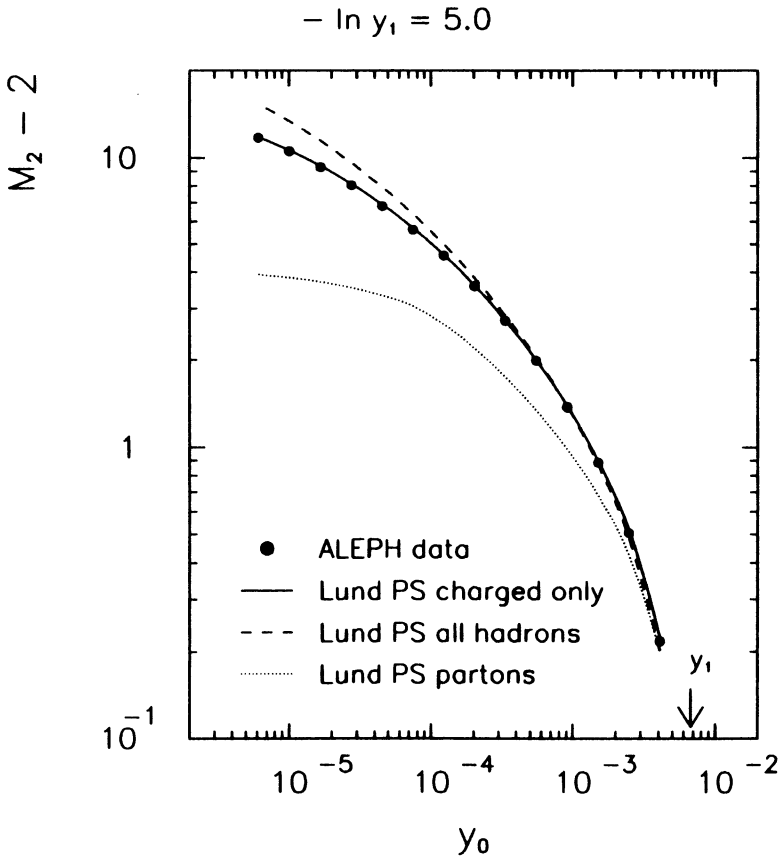
− ln y₁ = 5.0
M₂ − 2
10
1
10⁻¹
ALEPH data
Lund PS charged only
Lund PS all hadrons
Lund PS partons
y₁
10⁻⁵
10⁻⁴
10⁻³
10⁻²
y₀

Fig. 3c

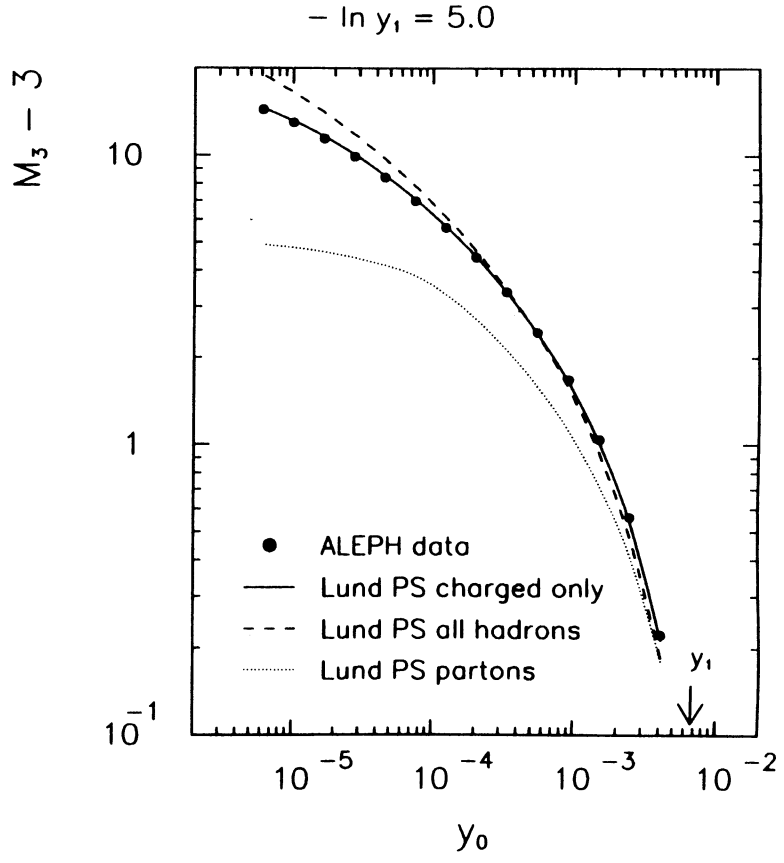
− ln y₁ = 5.0
M₃ − 3
10
1
10⁻¹
ALEPH data
Lund PS charged only
Lund PS all hadrons
Lund PS partons
y₁
10⁻⁵
10⁻⁴
10⁻³
10⁻²
y₀

Fig. 3d

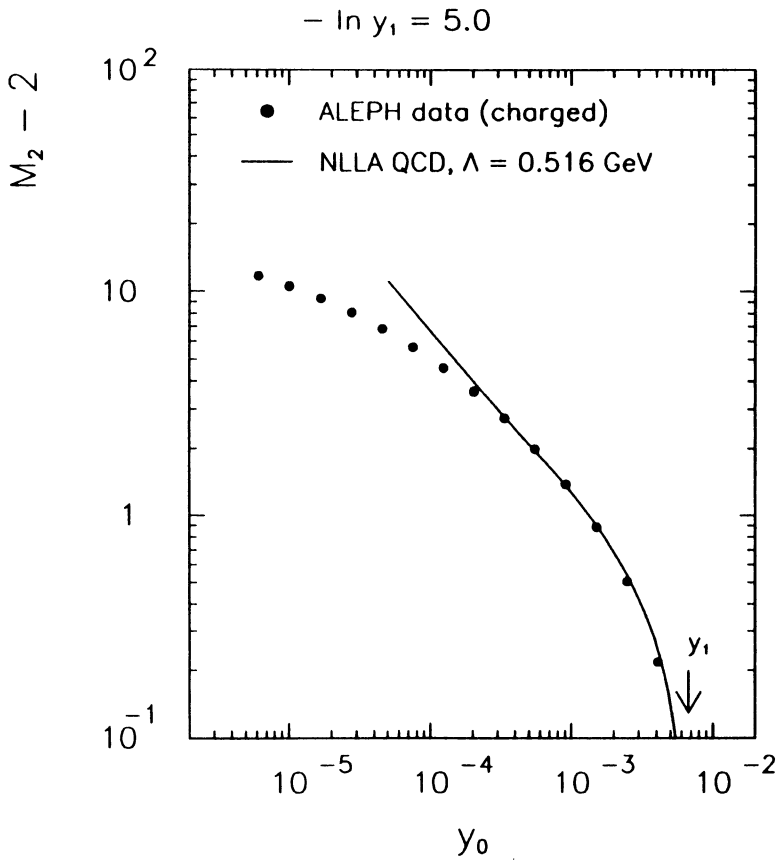
− ln y₁ = 5.0
M₂ − 2
10²
10
1
10⁻¹
ALEPH data (charged)
NLLA QCD, Λ = 0.516 GeV
y₁
10⁻⁵
10⁻⁴
10⁻³
10⁻²
y₀

Fig. 4a

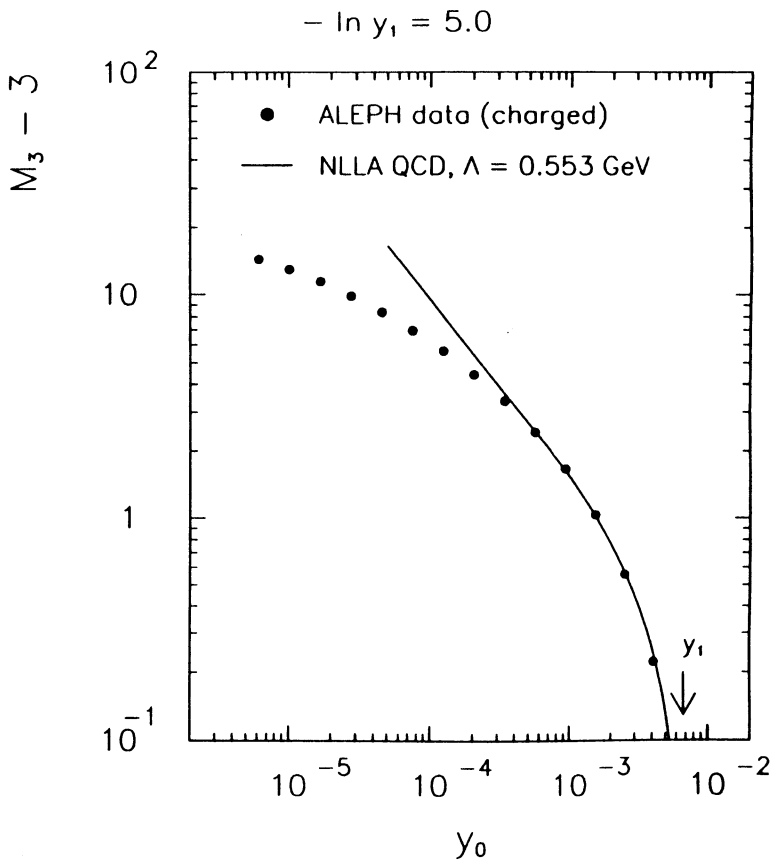
− ln y₁ = 5.0
M₃ − 3
10²
10
1
10⁻¹
ALEPH data (charged)
NLLA QCD, Λ = 0.553 GeV
y₁
10⁻⁵
10⁻⁴
10⁻³
10⁻²
y₀

Fig. 4b

Figure 5

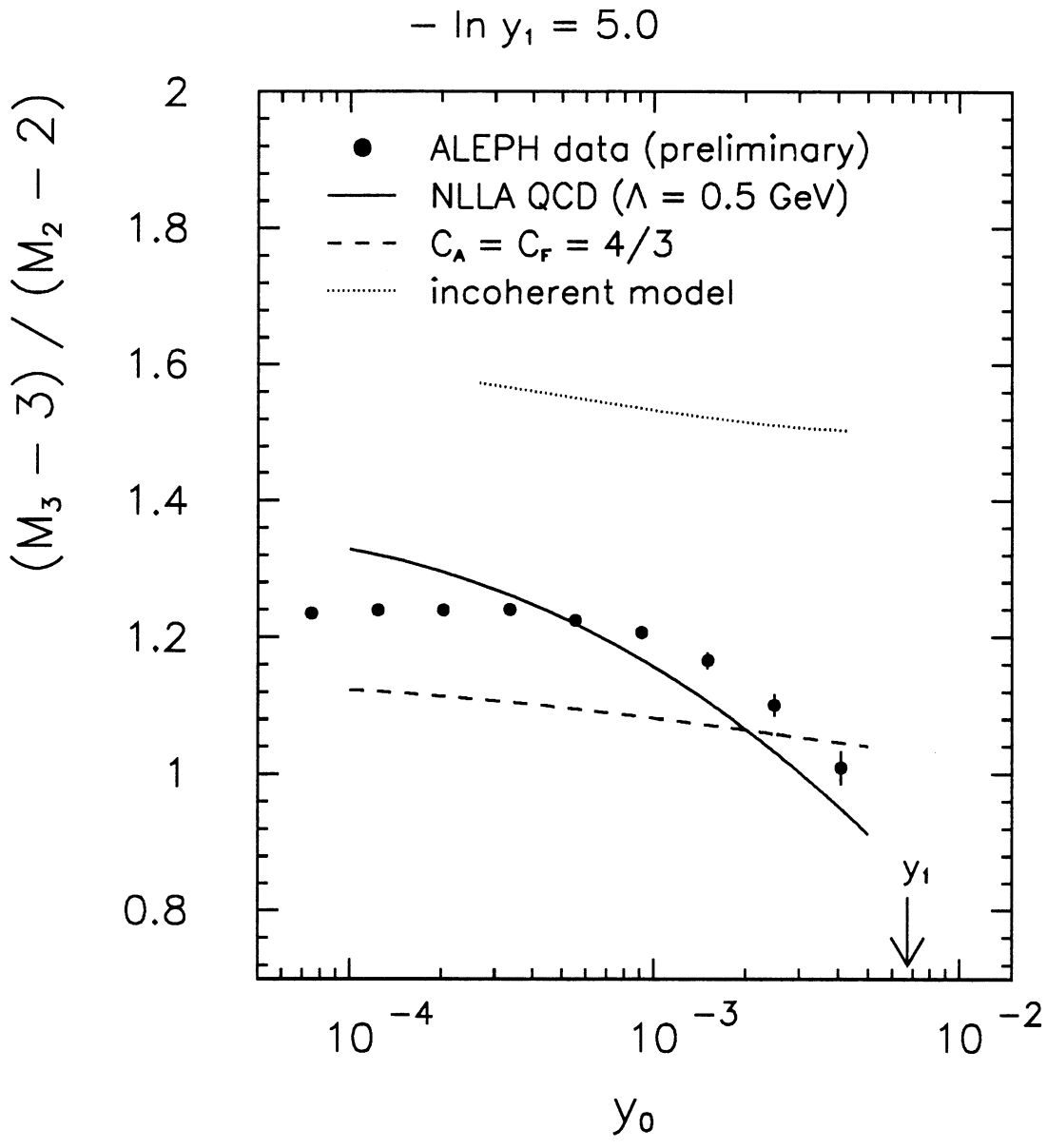
− ln y1 = 5.0
(M3 − 3) / (M2 − 2)
2
1.8
1.6
1.4
1.2
1
0.8
ALEPH data (preliminary)
NLLA QCD (Λ = 0.5 GeV)
CA = CF = 4/3
incoherent model
y1
10 −4
10 −3
10 −2
y0

Figure 6a

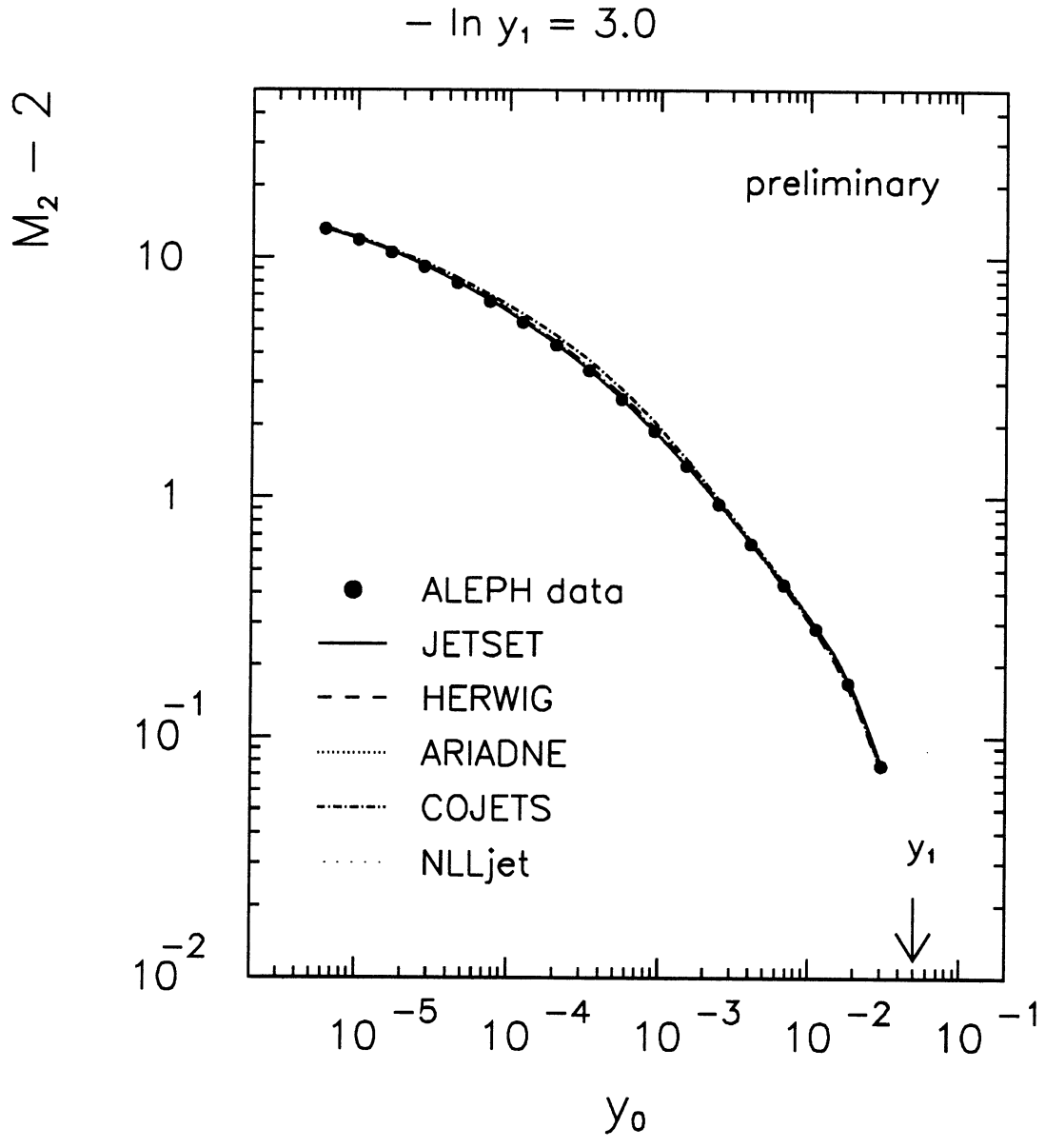
$-\ln y_1 = 3.0$
$M_2 - 2$
preliminary
ALEPH data
JETSET
HERWIG
ARIADNE
COJETS
NLLjet
y_1
10^{-1}
10^{-2}
10^{-5}
10^{-4}
10^{-3}
10^{-2}
10^{-1}
y_0

Figure 6b

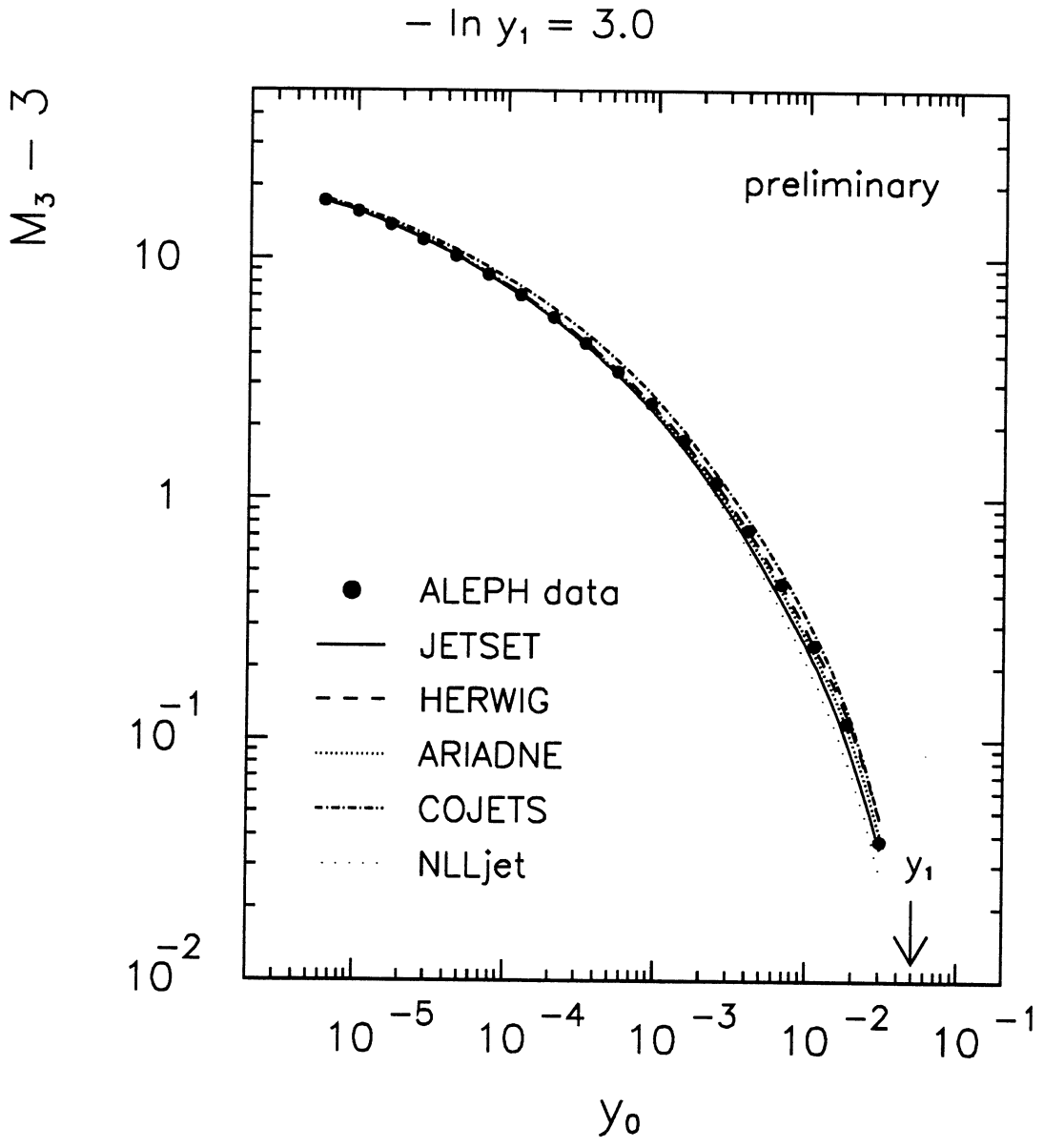
$-\ln y_1 = 3.0$
$M_3 - 3$
preliminary
10
1
10^{-1}
10^{-2}
ALEPH data
JETSET
HERWIG
ARIADNE
COJETS
NLLjet
y_1
10^{-5}
10^{-4}
10^{-3}
10^{-2}
10^{-1}
y_0

Figure 7a

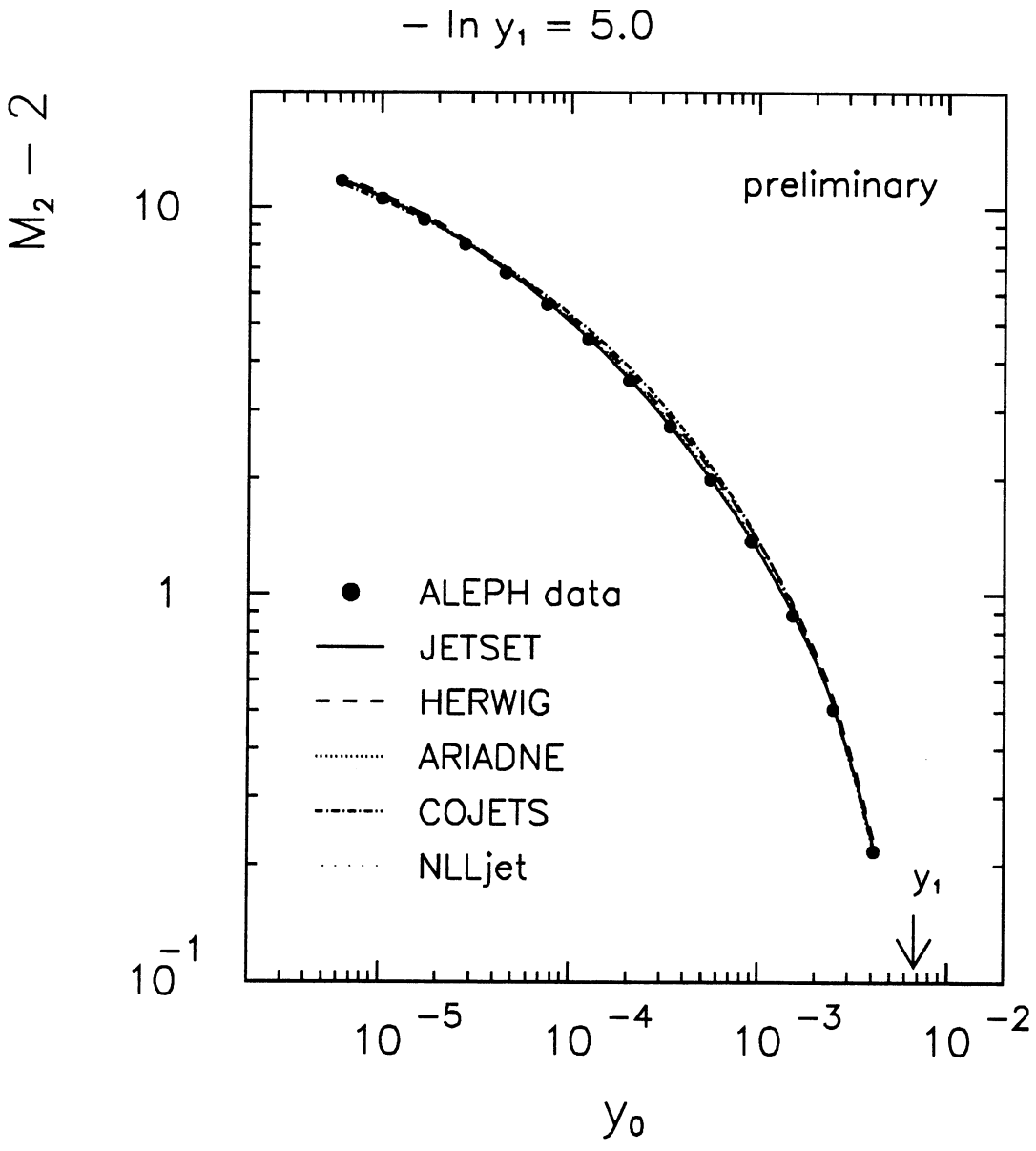
$-\ln y_1 = 5.0$
$M_2 - 2$
10
1
10^{-1}
preliminary
ALEPH data
JETSET
HERWIG
ARIADNE
COJETS
NLLjet
y_1
10^{-5}
10^{-4}
10^{-3}
10^{-2}
y_0

Figure 7b

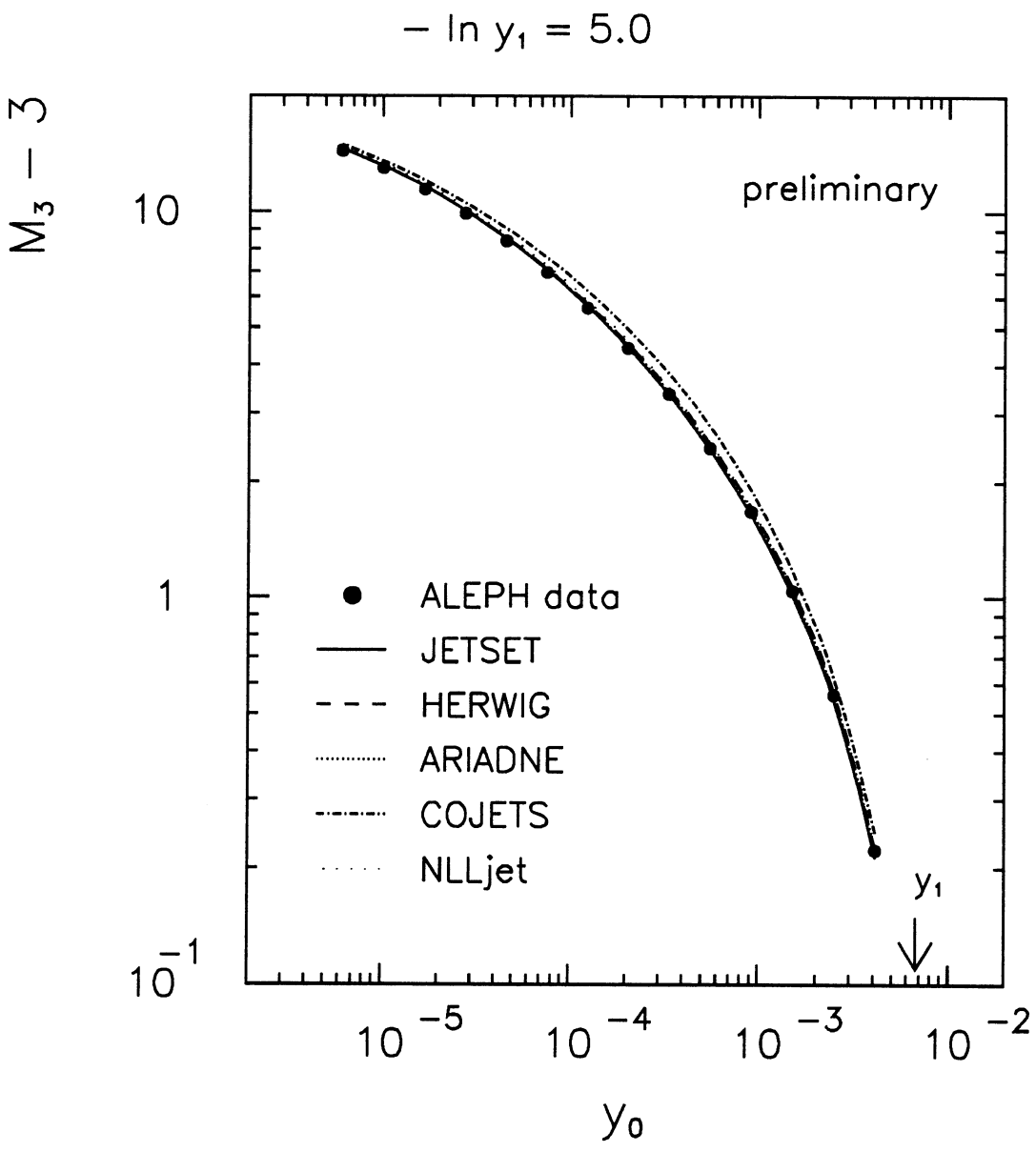
$-\ln y_1 = 5.0$
$M_3 - 3$
10
1
10^{-1}
preliminary
ALEPH data
JETSET
HERWIG
ARIADNE
COJETS
NLLjet
y_1
10^{-5}
10^{-4}
10^{-3}
10^{-2}
y_0

Figure 8a

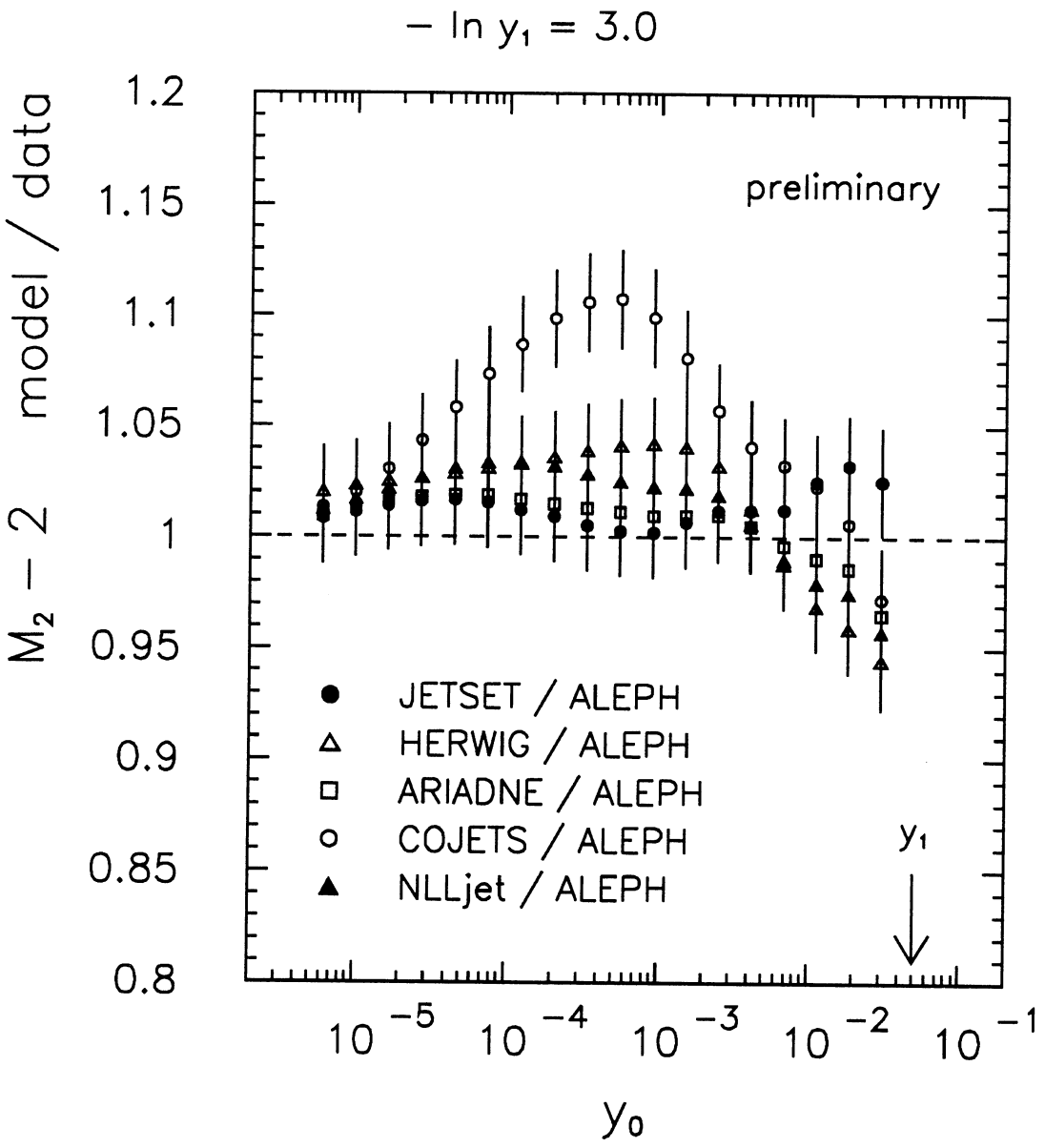
− ln y1 = 3.0
preliminary
M2 − 2 model / data
1.2
1.15
1.1
1.05
1
0.95
0.9
0.85
0.8
JETSET / ALEPH
HERWIG / ALEPH
ARIADNE / ALEPH
COJETS / ALEPH
NLLjet / ALEPH
y1
10 −5
10 −4
10 −3
10 −2
10 −1
y0

Figure 8b

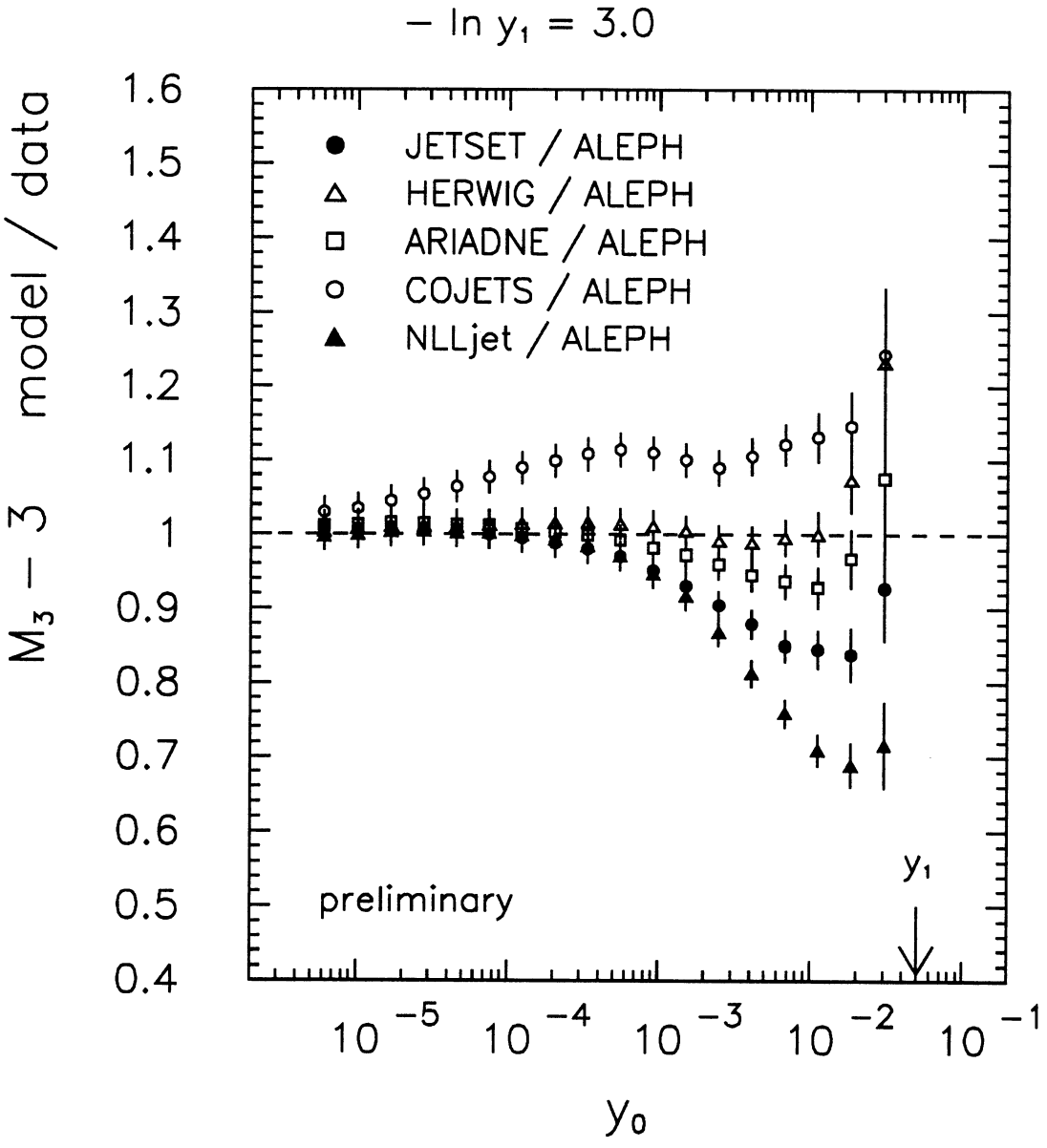
− ln y₁ = 3.0
M₃ − 3 model / data
1.6
1.5
1.4
1.3
1.2
1.1
1
0.9
0.8
0.7
0.6
0.5
0.4
JETSET / ALEPH
HERWIG / ALEPH
ARIADNE / ALEPH
COJETS / ALEPH
NLLjet / ALEPH
preliminary
y₁
10 −5
10 −4
10 −3
10 −2
10 −1
y₀

Figure 9a

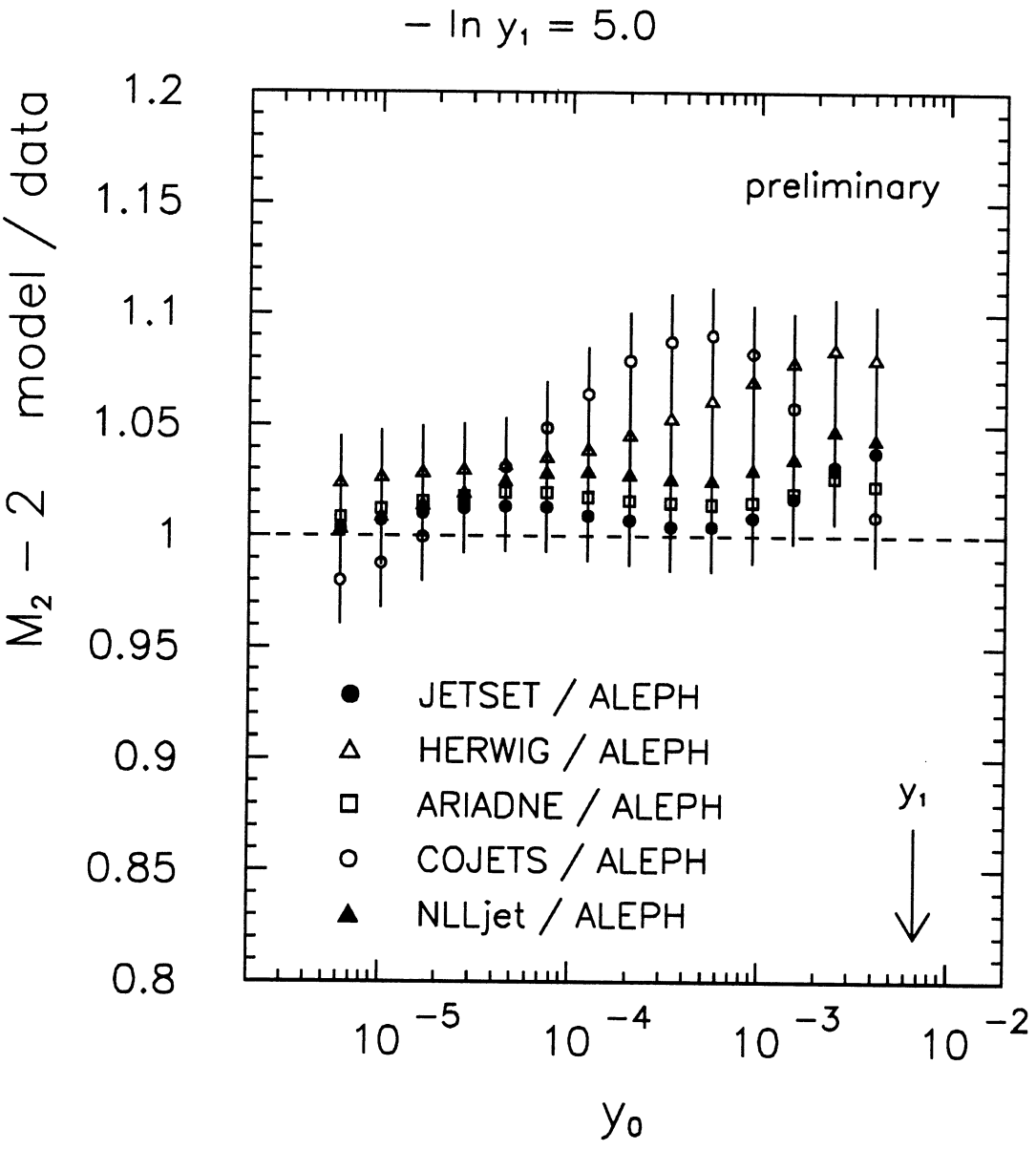
− ln y₁ = 5.0
M₂ − 2 model / data
1.2
1.15
1.1
1.05
1
0.95
0.9
0.85
0.8
preliminary
JETSET / ALEPH
HERWIG / ALEPH
ARIADNE / ALEPH
COJETS / ALEPH
NLLjet / ALEPH
y₁
10 −5
10 −4
10 −3
10 −2
y₀

Figure 9b

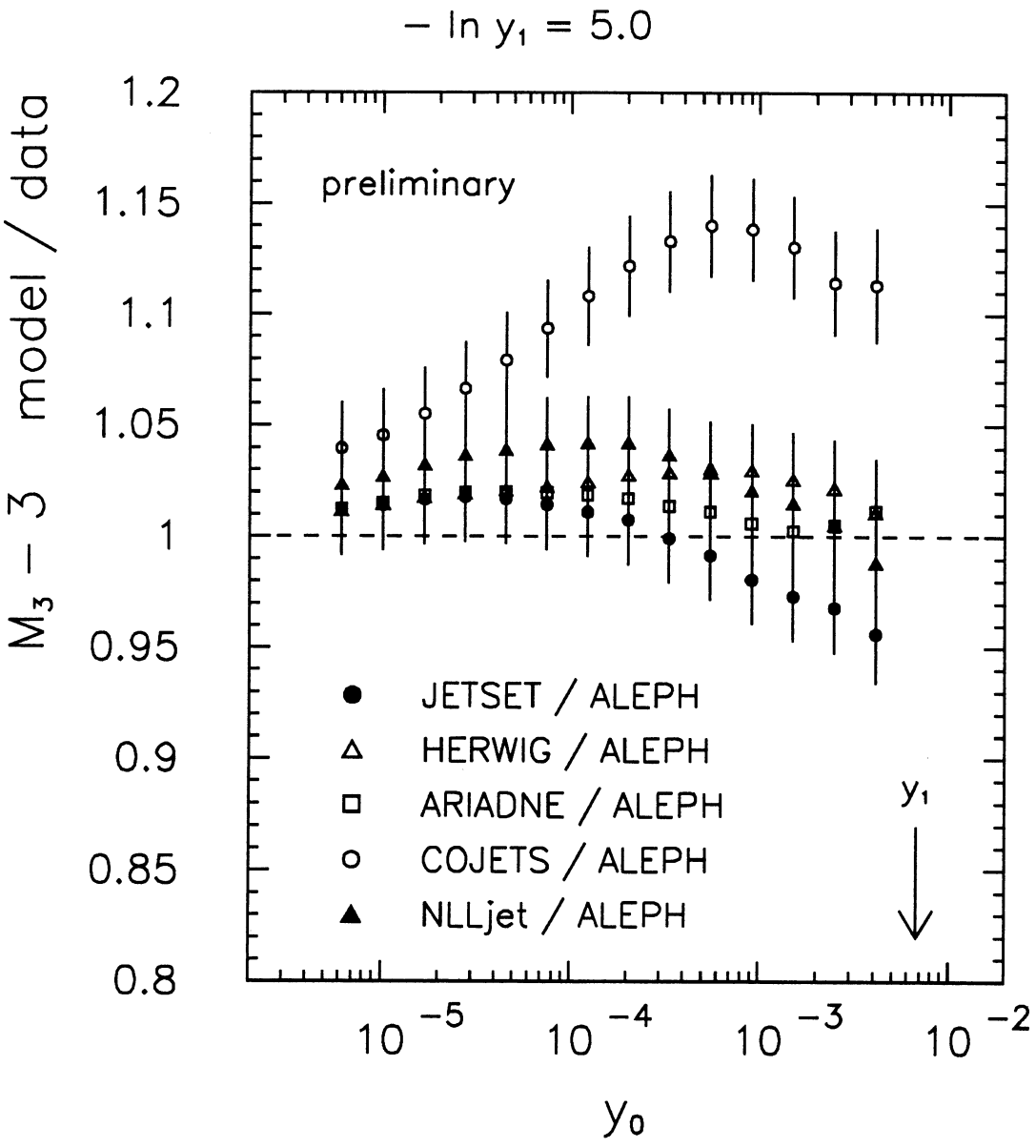
− ln y₁ = 5.0
M₃ − 3 model / data
1.2
1.15
1.1
1.05
1
0.95
0.9
0.85
0.8
preliminary
JETSET / ALEPH
HERWIG / ALEPH
ARIADNE / ALEPH
COJETS / ALEPH
NLLjet / ALEPH
y₁
10 −5
10 −4
10 −3
10 −2
y₀

Figure 10

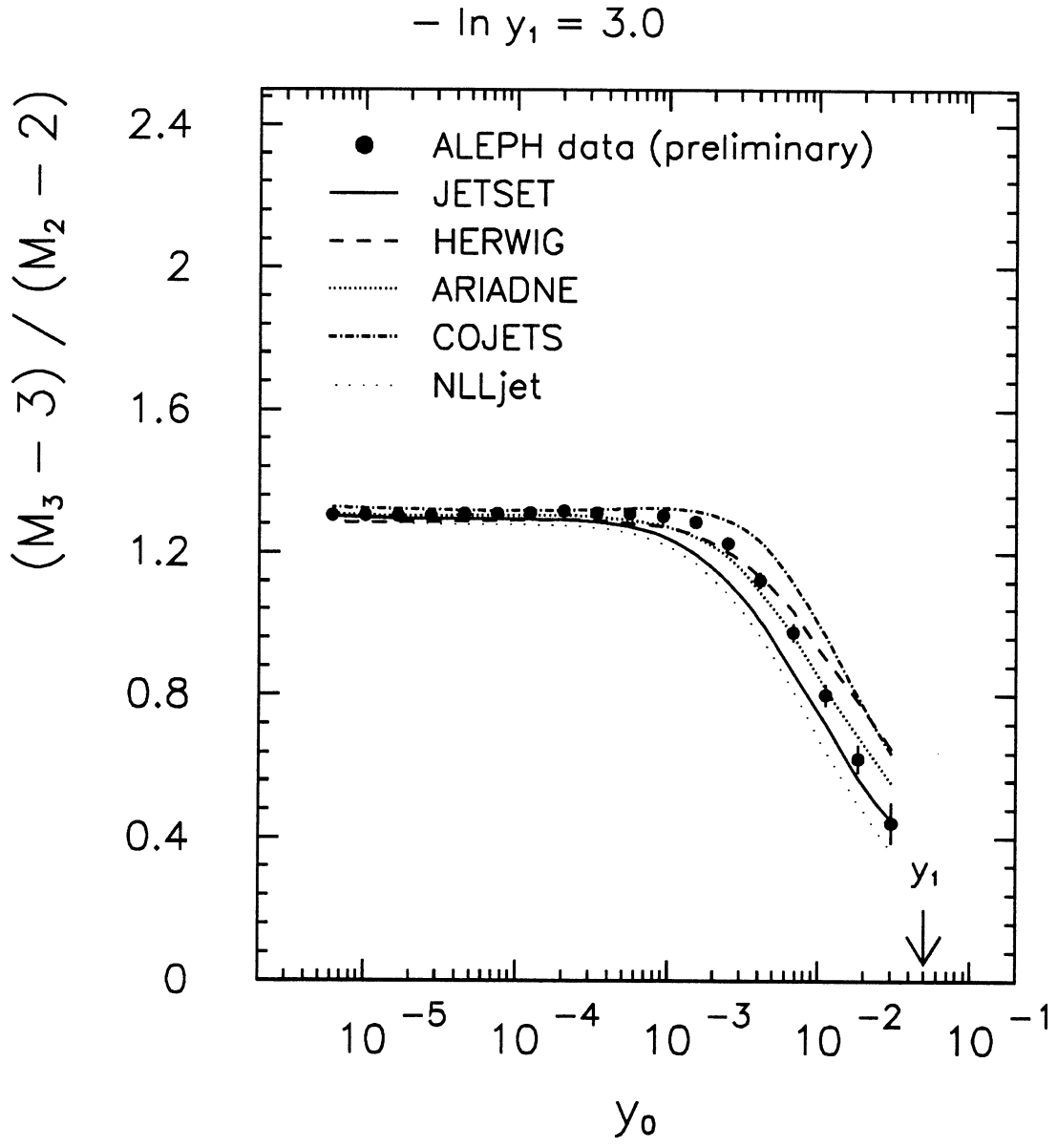
− ln y1 = 3.0
(M3 − 3) / (M2 − 2)
2.4
2
1.6
1.2
0.8
0.4
0
ALEPH data (preliminary)
JETSET
HERWIG
ARIADNE
COJETS
NLLjet
y1
10 −5
10 −4
10 −3
10 −2
10 −1
y0

Figure 11

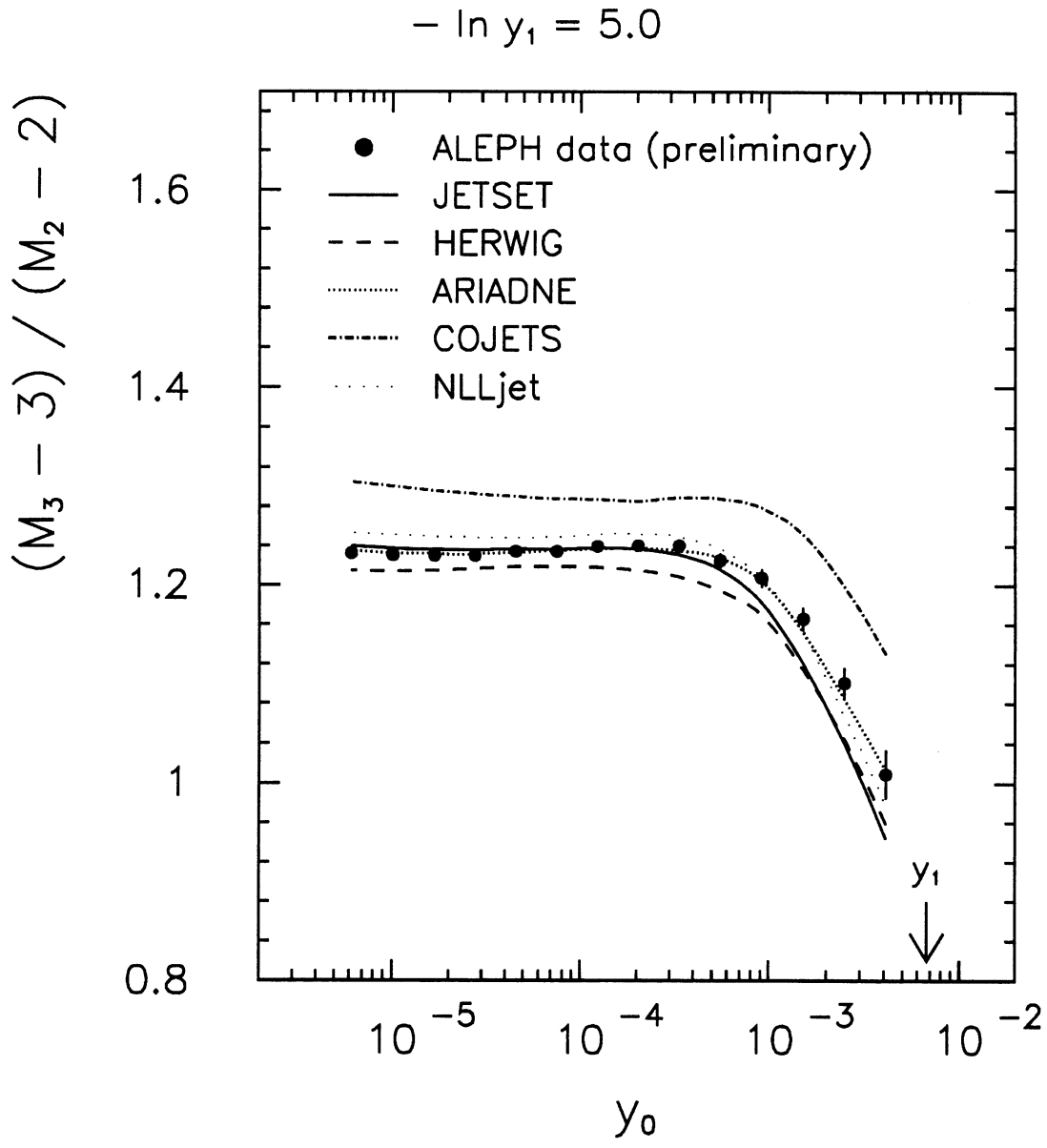
− ln y1 = 5.0
(M3 − 3) / (M2 − 2)
1.6
1.4
1.2
1
0.8
ALEPH data (preliminary)
JETSET
HERWIG
ARIADNE
COJETS
NLLjet
y1
10 −5
10 −4
10 −3
10 −2
y0